Korean J. of Chem. Eng., **11**(3), 198-203 (1994)

THERMODYNAMIC AND STRUCTURAL PROPERTIES OF HARD-SPHERE FLUIDS CONFINED WITHIN A SPHERICAL HARD-WALL PORE

Soong-Hyuck Suh† and Heai-Ku Park

Dept. of Chem. Eng., Keimyung University, Taegu 704-701, Korea
(Received 5 January 1994 • accepted 8 March 1994)

Abstract—The grand canonical ensemble Monte Carlo simulations have been carried out to investigate the thermodynamic and structural properties of hard-sphere fluids confined within a spherical hard-wall pore. Equilibrium partition coefficients and pore density profiles are computed over a wide range of particle-to-pore size ratios and concentrations distributing between an external bulk phase and a pore phase. The simulation data for equilibrium partitioning are used to assess the limitations and applicabilities of theoretical approximations including the virial expansion equation and the extended two-state prediction. The Monte Carlo results obtained in these studies, in conjunction with the theoretical models, provide the basis for a discussion on the steric effects in size-exclusion partitioning of such systems.

INTRODUCTION

Quantitative prediction of partitioning or distribution equilibrium is often necessary for the design of units in the chemical processes, including such areas as gel-permeation chromatography, membrane separation and transport, and adsorption processes using heterogeneous catalysis. The magnitude of partitioning into porous media may significantly differ from one system to another. One of the most important contributions to equilibrium partitioning is the steric exclusion effect between one molecule and the external pore wall. In addition, the presence of adsorption force fields influences equilibrium partitioning, particularly when the fluid is gas or vapor. In such cases the attractive interaction can enhance the degree of partitioning whereas the repulsive interaction will reduce the partition coefficient.

Although the concept of size-exclusion partitioning was recognized many years ago [1], it was only comparatively recent that theoretical equations have been developed and applied for pore systems. Following from the pioneering work of Giddings et al. [2], there are several theoretical equations based on statistical mechanical approximations. Currently, the different approaches to this subject may be classified as (i) virial expansions [3-7], (ii) integral equation theories [8-10], and (iii) density functional approximations [11-13]. A comprehensive review in this area is provided by Deen [14], and more recently by Fanti [15].

Reliable and unambiguous results have become increasingly necessary to eliminate any underlying uncertainties involved in various theoretical approaches. One of the most widely used model pores in these studies is a geometrically ideal pore such as a slit, cylindrical, or spherical one. The simplest possible model potential is that of a hard-sphere fluid combined with only sterically exclusive hard-wall interactions. However, the present level of modeling achievements in this area is far too crude to allow direct comparison with real laboratory experiment. Consequently, as an intermediate between theory and experiment, molecular-based computer simulations have proved to be an extremely useful diagnostic tool. In principle such machine experiment (computer simulation) can represent essentially 'exact' experimental data for precisely defined model systems.

In the present work, we investigate the thermodynamic and structural properties of confined hard-sphere fluids inside a structureless spherical hard-wall pore. To this end, grand canonical ensemble Monte Carlo (GCEMC) simulations have been carried out over a wide range of pore fluid concentrations and particle-to-pore size ratios. A simple pore model is

†To whom all correspondences to be addressed.

used to elucidate the most important features governing the size-exclusion partitioning in a spherical cavity. Our simulation results can also provide a basis to discuss whether or to what extent theoretical approximations appearing in the literature can be applied to predict the equilibrium properties of such systems.

EQUILIBRIUM PARTITIONING

The partition coefficient, K, is defined as the ratio of the average concentration in the pore phase to that in the external bulk phase under equilibrium conditions:

$$K=\frac{n_p}{n_b} \tag{1}$$

where the subscripts p and b refer to the pore and the bulk phase, respectively.

Since the bulk and the pore fluids are in equilibrium, the chemical potentials are the same in both phases:

$$\mu_b=\mu_p \tag{2}$$

Choosing the ideal gas state of unit activity and fixed temperature as the standard state, the chemical potentials for both phases can be written as

$$\mu_b=\mu^o+kT\ \ln\ (\gamma_b\ n_b) \tag{3}$$

and

$$\mu_p=\mu^o+kT\ \ln\left(\frac{V_p\ \gamma_p\ n_p}{V_{p,eff}}\right) \tag{4}$$

where k is the Boltzmann constant and γ is the activity coefficient. V_p and $V_{p,eff}$, respectively, denote the total pore volume and the effective pore volume accessible to the single pore particle.

From Eq. (1) through Eq. (4) one may find

$$K=\frac{V_{p,eff}}{V_p}\ \frac{\gamma_b}{\gamma_p} \tag{5}$$

The equilibrium partition coefficient expressed in this equation is a general expression for a given pore system.

In the virial-type approaches [3-7], the ratio of the activity coefficients in Eq. (5) can be written as a series expansion in powers of the reduced bulk concentration n_b^*:

$$K=K_o(1+\alpha_1\ n_b^*+\alpha_2\ n_b^{*2}+\cdots) \tag{6}$$

The leading term, K_o, directly corresponds to the Henry's law constant at infinite dilution resulting from particle-pore wall interactions alone. Computations are simplest in this Henry's law limit where interactions among pore particles become negligible. In the case of rigid particles inside impenetrable hard-wall pores, the center of a particle cannot be closer to the pore wall than the wall contact distance. As a result, in the systems of hard-sphere fluids within geometrically well-defined pores, the Henry's law constant is simply given by

$$K_o=\frac{V_{p,eff}}{V_p}=(1-\lambda)^n \tag{7}$$

where λ is the particle-to-pore size ratio and n=1, 2, or 3 for the infinite slit, cylindrical, or spherical pores, respectively.

α_1, α_2, etc., appearing in Eq. (6) represent the virial coefficients arising from the interaction of clusters of two, three, etc., pore particles with the pore wall. For a one-component hard-sphere fluid trapped in a slit, cylindrical, and spherical pore, the first and second virial coefficients, α_1 and α_2, can be evaluated within the framework of the statistical mechanics [3-5]. The results obtained for the first virial coefficient are essentially exact. However, the second virial coefficient must be calculated numerically, e.g. with the aid of the Percus-Yevick approximation in order to avoid the complex configurational integral of three particles simultaneously interacting with each other and with the pore wall. An obvious trend is that the higher order terms in the virial expansion increase in computational complexity, and direct calculations are very difficult even for simple pore geometries.

THE GCEMC SIMULATION METHOD

We consider a system of a hard-sphere fluid with molecules of diameter σ inside a structureless spherical hard-wall pore of diameter d_p. The fluid-fluid, ϕ_{ff}, and the fluid-wall interactions, ϕ_{fw}, can be expressed as

$$\phi_{ff}(r)=\begin{cases}\infty, & r>\sigma\\ 0, & r<\sigma\end{cases} \tag{8}$$

and

$$\phi_{fw}(r)=\begin{cases}\infty, & r>R_{p,eff}\\ 0, & r<R_{p,eff}\end{cases} \tag{9}$$

where $R_{p,eff}$ represents the effective pore radius, i.e., $(d_p-\sigma)/2$.

The fluid inside the pore is in equilibrium with the bulk fluid. In the grand canonical ensemble itself, the

chemical potential μ, the total volume V, and the temperature T of the system are fixed. Since the number of fluid particles is allowed to fluctuate in this μVT-ensemble, the GCEMC calculation is most appropriate for determining the partition coefficient for the systems to be studied [16, 17]. Asymmetric GCEMC sampling, proposed by Adams [18, 19], consists of two independent steps. In the first step, a randomly chosen particle is moved within a given maximum displacement. The move is either accepted or rejected subject to the potential energy change. This procedure is exactly the same as the conventional canonical ensemble Monte Carlo method. The second step proceeds to attempt an addition or removal of a particle. The success of either an addition or removal is controlled both by the potential energy change and by the chemical potential parameter. This compound event is repeated as many times as is desired and the equilibrium properties of the systems are evaluated at each step.

Computations for the bulk hard-sphere fluid were not required since the chemical potential in Eq. (2), or conversely the activity coefficient in Eq. (3), at any given concentration can be calculated with sufficient accuracy using the Carnahan-Starling equation of state [20]:

$$\frac{\mu-\mu^{o}}{kT}=\frac{\eta(8-9\eta+3\eta^{2})}{(1-\eta)^{3}} \tag{10}$$

where $\eta=(6/\pi)\,n_b^*$ is the hard-sphere packing fraction and $n_b^*=n_b\sigma^3$ is the reduced bulk number density.

The initialization procedure adopted here was to construct the simulated pore model, devoid of fluid particles, and then proceed directly to the GCEMC algorithm of the hard-sphere fluid [18]. During the initial stages of a simulation the configurations generated were not representative of the equilibrium ensemble and were discarded from the averaging process. In all cases studied here configurations were equilibrated for 2-4 million steps before accumulating data. The resulting ensemble averages were obtained during the final 40-80 million simulation steps.

RESULTS AND DISCUSSION

In Fig. 1 we illustrate the concentration dependencies on size-exclusion partitioning for the particle-to-pore size ratios, $\lambda=0.2$ and $\lambda=0.4$. The resulting partition coefficients obtained from the GCEMC computations are shown as a function of bulk concentrations. Also shown in this figure as solid curves are theoretical predictions using the virial-type expansions given

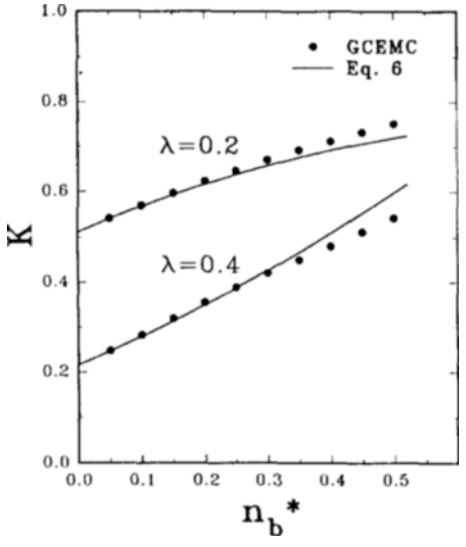

Fig. 1. Partition coefficient as a function of n_b^* for $\lambda=0.2$ and $\lambda=0.4$.

in Eq. (6), in which terms up to order of n_b^{*2} are included. To date, this virial expression has been moderately successful in explaining the concentration effects for the equilibrium partitioning of inert, noninteracting solute systems. For the systems studied here, the agreement with the GCEMC results is seen to be good in lower concentrations $n_b^*\leq 0.3$.

The partition coefficients calculated using this truncated virial expansion, however, depart from the simulation results with increasing bulk fluid concentrations. Furthermore, the limited form of the three-term virial expansion in Eq. (6) can either underestimate or overestimate K-values depending on the values of λ and n_b^*. The poor agreement with the GCEMC calculations for higher bulk concentrations is primarily due to the omitted terms of order of n_b^{*3} or greater. In addition, as mentioned earlier, the theoretical results for α_2 calculated by Glandt [3, 4] and Anderson and Brannon [5] are based on the Percus-Yevick approximation. This approximation was found to be inaccurate particularly at the high concentration regime; for example, the second virial coefficient was underestimated by as much as 35% for narrow cylindrical pores [5]. In this case, the much greater influence exerted by the pore wall on the structure of the pore fluid than might be inferred from this approximation can be expected.

In the previous simulation work for systems of cylindrical pores [21-23], the size-exclusion effect was explained in terms of the work required to create a

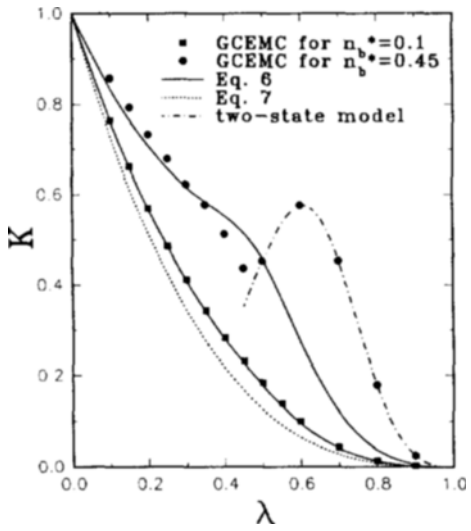

Fig. 2. Partition coefficient as a function of λ for $n_b^*=0.1$ and $n_b^*=0.45$.

cavity in the pore fluid. The degree of partitioning was observed to be very sensitive to the local pore density in the vicinity of the pore wall. In equilibrium partitioning, the partition coefficient is primarily determined by configurational entropy differences between the bulk and the pore fluid phase. Under these conditions one may expect the local molecular configuration in the grand canonical ensemble to play an important role in size-exclusion partitioning.

A physical interpretation of this observation follows from thermodynamic arguments similar to those used in the scaled particle theory [24]. An alternative form for the partition coefficient can be written as

$$K=(1-\lambda)^3 \exp\left[-\frac{W_p(\lambda)-W_b(\lambda)}{kT}\right] \quad (11)$$

where $W_p(\lambda)$ and $W_b(\lambda)$ are the reversible work to create a cavity of size λ in the pore and the bulk phase, respectively.

The results in Figs. 2 and 3 demonstrate this last point more clearly. In Fig. 2, the two sets of the GCEMC runs at the fixed bulk concentrations of $n_b^*=0.1$ and $n_b^*=0.45$ were carried out over wider ranges of λ-values. The amount of cavity work required to accommodate a particle in the pore fluid increases rapidly with the increment of λ-values, and this leads to a significant reduction of size-exclusion partitioning. For the sufficiently dilute systems, particle-particle interactions become negligible, and, for any given values of λ, the reversible cavity work in the pore phase approaches that in the bulk phase. In the limit of $n_b^*\to 0$, the partition coefficient expressed in Eq. (11) is simply reduced to the Henry's law constant K_o as given in Eq. (7), i.e., $(1-\lambda)^3$.

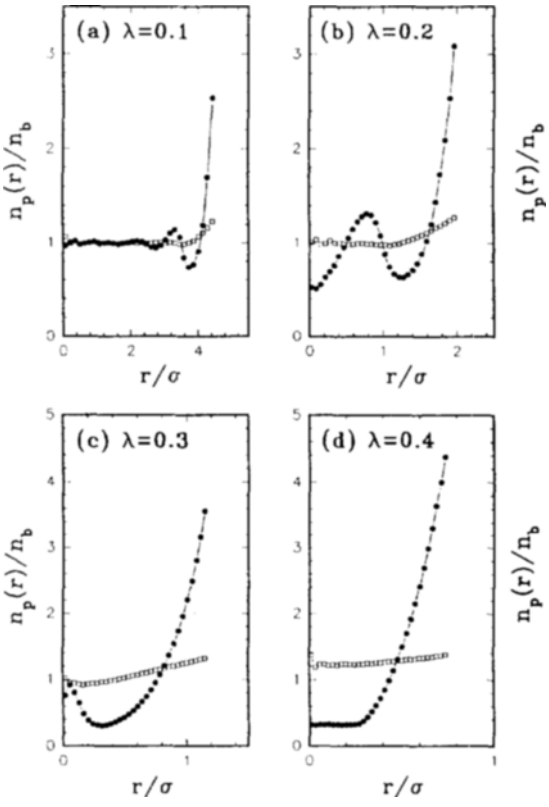

Fig. 3. Normalized pore density profile as a function of r/σ.
The open squares and the filled circles correspond to the systems of $n_b^*=0.1$ and $n_b^*=0.45$, respectively.

As we increase bulk concentrations, the Henry's law constant shown as the dotted curve in Fig. 2 is no longer valid even for the dilute bulk concentration of $n_b^*=0.1$. Obviously, the concentration effects are more profound in the case of $n_b^*=0.45$. The breakdown of the Henry's law results from density inhomogeneities in the pore fluid. The resulting partition coefficients predicted by theoretical virial expansions for the dilute concentration ($n_b^*=0.1$) are observed to be in reasonable agreement with the corresponding GCEMC results. In contrast, significant deviations from theory were noted for the higher concentration regime ($n_b^*=0.45$). This is again partly due to an inaccurate evaluation of the second virial coefficients via the Per-

cus-Yevick approximation employed in virial expansion equations.

In the range $0.5<\lambda<1.0$ only two occupancy states are permissible since the accessible pore region can be occupied by zero or one particle. In this case the average occupation number of particles in equilibrium with an external bulk fluid can be exactly calculated using the two-state Markov chain processes [25]. The chain-dotted curve in Fig. 2 represents the partition coefficients obtained from the extended two-state model. For $\lambda>0.5$ the excellent agreement with simulation results confirms the validity of this model. For the systems of higher concentrations, configurations occupied by one particle become more probable in the grand canonical ensemble. It may be shown, using this extended two-state model, that the local maximum moves upward to the right towards $\lambda\rightarrow1.0$ as the bulk concentration increases. As the concentration decreases, however, this peak will be gradually diminished, and eventually disappears in the ideal gas limit, $n_b^* \rightarrow 0$.

In Fig. 3 we have plotted the pore density profiles scaled to the corresponding bulk concentration, $n_p(r)/n_b$, for a few selected runs to illustrate the manner in which the local pore densities change with increasing λ-values. The open squares and the filled circles, respectively, correspond to the normalized density profiles inside a spherical hard-wall pore for the systems of $n_b^*=0.1$ and $n_b^*=0.45$. Pore profiles for $\lambda>0.5$ are not displayed in this paper since the resulting profiles are constant over the pore volume. In this case there is a uniform probability of finding the center of one particle in the pore phase where the external potential is zero.

The average pore densities for $n_b^*=0.1$ are close to those of the bulk system. As concentration increases, however, density oscillations arise inside the pore with a wavelength of the order of the particle size. Such density inhomogeneities exhibited in Fig. 3 primarily result from the shielding effect in the immediate vicinity of the pore walls. In the case of $\lambda=0.2$ and $n_b^*=0.45$, for example, the pore fluid forms a double-layered structure with the higher peak near the wall, while a monolayer pore structure extending two particles across the pore diameter is predominant for $\lambda=0.4$ and $n_b^*=0.45$. This result is attributed to the fact that confined hard-sphere fluids in a spherical pore experience the structural reordering in the vicinity of the pore wall even though the energetic interaction considered here is only steric exclusion. The above observations are not restricted to hard-sphere fluids. Equilibrium partitioning and pore structural properties similar to those illustrated in Figs. 2 and 3 have been shown to exist for Lennard-Jones fluids trapped in two slit pores [26] and cylindrical pores [11, 23]. The magnitude of partitioning in adsorbing systems of cylindrical pores was also found to be qualitatively close to the corresponding results for the hard-sphere systems [21, 22].

CONCLUSION

In the present paper we have reported the computer simulation results via the grand canonical ensemble Monte Carlo method to investigate the thermodynamic and structural properties of hard-sphere fluids confined within a spherical hard-wall. The accuracy of the virial expansion for size-exclusion partitioning, taken to terms of order n_b^{*2}, is limited to bulk phase concentrations less than 0.3. As the particle size approaches the pore size, the range of applicability of this approximation is further reduced. In this limit, the extended two-state model is very reliable for predicting K-values for the entire range of bulk concentrations. The equilibrium and structural properties obtained in this work can be used as a convenient reference for more sophisticated real systems. Although this simple spherical pore model represents only the conceptual nature of ideal pores, the pore-size and concentration effects can be useful in the study of zeolitic pore systems. In practice the geometry of many zeolite cavities closely resembles a spherical model pore. Our simulation results, in conjunction with previous simulation studies using more realistic model potentials [27, 28], will provide useful insight into the microscopic behavior of fluids adsorbed in zeolite pores. In the high-temperature limit, the effect of the attractive force field becomes negligible so that our simulation results for hard-sphere interactions can be reasonable approximations for such real systems.

ACKNOWLEDGEMENT

This research was supported by NON DIRECTED RESEARCH FUND, Korea Research Foundation (1993). SHS wishes to thank Mr. Woo-Chul Kim in implementing simulation data during this work.

NOMENCLATURE

d_p : spherical pore diameter
k : Boltzmann constant
K : partition coefficient
K_∞ : partition coefficient at infinite dilution

n : number density
r : relative distance or radial position
$R_{p,eff}$: effective pore radius
T : absolute temperature
V : volume
$V_{p,eff}$: effective pore volume
W(λ) : reversible work required to create a cavity of size λ

Greek Letters

α_1,α_2 : first and second virial coefficient
γ : activity coefficient
η : hard-sphere packing fraction
λ : particle-to-pore size ratio
μ : chemical potential
μ^o : standard chemical potential
σ : hard-sphere diameter
φ : potential interaction

Subscripts

b : bulk phase
ff : fluid-fluid
fw : fluid-pore wall
p : pore phase

Superscript

* : reduced quantity

REFERENCES

1. Ferry, J. D.: *J. Gen. Physiol.*, **20**, 95 (1936).
2. Giddings, J. C. E., Kucera, E., Russel, C. P. and Myers, M. N.: *J. Phys. Chem.*, **72**, 4397 (1968).
3. Glandt, E. D.: *J. Coll. Interface Sci.*, **77**, 512 (1980).
4. Glandt, E. D.: *AIChE J.*, **27**, 51 (1981).
5. Anderson, J. L. and Brannon, J. H.: *J. Polymer Sci.*, **19**, 405 (1981).
6. Mitchell, B. D. and Deen, W. M.: *J. Membrane Sci.*, **19**, 75 (1984).
7. Post, A. J. and Glandt, E. D.: *J. Coll. Interface Sci.*, **108**, 31 (1985).
8. Zhou, Y. and Stell, G.: *Mol. Phys.*, **66**, 767 (1989).
9. Zhou, Y. and Stell, G.: *Mol. Phys.*, **66**, 791 (1989).
10. Sloth, P.: *J. Chem. Phys.*, **93**, 1292 (1990).
11. Peterson, B. K., Gubbins, K. E., Heffelfinger, G. S., Marini Bettolo Marconi, U. and van Swol, F.: *J. Chem. Phys.*, **88**, 6487 (1988).
12. Post, A. J.: *J. Coll. Interface Sci.*, **129**, 451 (1989).
13. Calleja, M., North, A. N., Powles, J. G. and Rickayzen, G.: *Mol. Phys.*, **23**, 973 (1991).
14. Deen, W. M.: *AIChE J.*, **33**, 1409 (1987).
15. Fanti, L. A.: Ph. D. Dissertation, University of Pennsylvania, PA (1989).
16. Nicholson, D. and Parsonage, N. G.: "Computer Simulation and the Statistical Mechanics of Adsorption", Academic Press, New York (1982).
17. Allen, M. P. and Tildesley, D. J.: "Computer Simulation of Liquids", Clarendon Press, Oxford (1987).
18. Adams, D. J.: *Mol. Phys.*, **28**, 1241 (1974).
19. Adams, D. J.: *Mol. Phys.*, **29**, 307 (1975).
20. Reed, T. M. and Gubbins, K. E.: "Applied Statistical Mechanics", McGraw-Hill, New York (1973).
21. MacElroy, J. M. D. and Suh, S.-H.: *AIChE Symp. Ser.*, **82**, 133 (1986).
22. Suh, S.-H. and MacElroy, J. M. D.: *Mol. Phys.*, **60**, 475 (1987).
23. MacElroy, J. M. D. and Suh, S.-H.: *Mol. Simul.*, **2**, 313 (1989).
24. Lebowitz, J. L., Helfand, E. and Praestgaard, E.: *J. Chem. Phys.*, **43**, 774 (1965).
25. Hoel, P., Port, S. C. and Stone, C. J.: "Introduction to Stochastic Processes", Houghton Mifflin Co., Boston (1972).
26. Magda, J. J., Tirrell, M. and Davis, H. T.: *J. Chem. Phys.*, **83**, 1888 (1985).
27. Razmus, D. M. and Hall, C. K.: *AIChE J.*, **37**, 769 (1991).
28. Woods, G. B. and Rowlinson, J. S.: *Chem. Soc. Farad. Trans. 2*, **85**, 765 (1989).